Two-dimensional maps at the edge of chaos: Numerical results for the Henon map

Ugur Tirnakli
Department of Physics, Faculty of Science, Ege University, 35100 Izmir, Turkey
tirnakli@sci.ege.edu.tr

The mixing properties (or sensitivity to initial conditions) of two-dimensional Henon map have been explored numerically at the edge of chaos. Three independent methods, which have been developed and used so far for the one-dimensional maps, have been used to accomplish this task. These methods are (i) measure of the divergence of initially nearby orbits, (ii) analysis of the multifractal spectrum and (iii) computation of nonextensive entropy increase rates. The obtained results strongly agree with those of the one-dimensional cases and constitute the first verification of this scenario in two-dimensional maps. This obviously makes the idea of weak chaos even more robust.

PACS Number(s): 05.45.-a, 05.20.-y, 05.70.Ce

Nowadays a growing number of works addressing one-dimensional dissipative maps signals out the increasing interest in exploring the behaviour of nonlinear dynamical systems at the edge of chaos [1–9]. This interest mostly stems from the fact that the standard theory considers this special point (and also all other points where the standard Lyapunov exponent vanishes) as *marginal* and works addressing directly these marginal points are less than the works on the other regions of the system. Recent works addressing the behaviour of dynamical systems at these points are based on the conjecture that the divergence of initially nearby trajectories, characterized by the sensitivity function

$$\xi(t) = \lim_{\Delta x(0)\to 0} \frac{\Delta x(t)}{\Delta x(0)} \tag{1}$$

(where $\Delta x(0)$ and $\Delta x(t)$ are the discrepancies of the initial conditions at times 0 and t), are not of the exponential type at these marginal points, but rather, of the power-law type like [2]

$$\xi(t) = [1 + (1-q)\lambda_q t]^{1/(1-q)} \qquad (q \in \mathcal{R}), \tag{2}$$

which comes from the conjecture that the controlling equation becomes $d\xi/dt = \lambda_q \xi^q$ (instead of the usual one $d\xi/dt = \lambda_1 \xi$). This result recovers the standard one in the $q \to 1$ limit and also defines a generalized version of the Lyapunov exponent λ_q, which inversely scales with time, but now within a power-law. Within this unified scheme, apart from the standard regimes where we have chaos, sensitivity and insensitivity to the initial conditions, we have also weak insensitivity to the initial conditions for $q > 1$, $\lambda_1 = 0$, $\lambda_q < 0$ and weak sensitivity to the initial conditions for $q < 1$, $\lambda_1 = 0$, $\lambda_q > 0$. The last case characterizes also the most interesting marginal point, the chaos threshold. This kind of asymptotic power-law sensitivity to the initial conditions has already been observed since long [10–12], but Eq.(2) provides a more complete description than that, since it is expected to be valid not only at very large times but also at intermediate times as well (of course after a short transient). This equation in fact corresponds to the power-law growth of the upper bounds of a complex time dependence of the sensitivity function, which includes considerable and ever lasting fluctuations. These upper bounds ($\xi(t) \propto t^{1/(1-q)}$) allow us to determine the proper value of the q index (say q^*) for the dynamical system under consideration. This constitutes the first method of finding the q^* value of a given dynamical system.

The second method for the same purpose is based on the geometrical aspects of the critical attractor of the system at the edge of chaos. Due to the complexity of critical dynamical attractor, a multifractal formalism is needed in order to reveal its complete scaling behaviour. In this formalism, each moment of the probability distribution has a contribution coming from a particular subset of points of the attractor with fractal dimension f. Using a partition containing M boxes, the content on each contributing box scales as $M^{-\alpha}$. The multifractal measure is then characterized by the continuous function $f(\alpha)$ which reflects the fractal dimension of the subset with singularity strength α [13,14]. Using the scaling behaviour of the multifractal singularity spectrum $f(\alpha)$, a new scaling relation has been proposed [3] as

$$\frac{1}{1-q^*} = \frac{1}{\alpha_{min}} - \frac{1}{\alpha_{max}} \qquad (q^* < 1) \tag{3}$$

where α_{min} and α_{max} are the vanishing points of downward parabolalike concave curve $f(\alpha)$ and characterize the scaling behaviour of the most concentrated and most rarefied regions on the attractor. This fascinating relation, which connects the power-law sensitivity of dynamical systems with purely geometrical quantities, establishes another independent method for estimating the q^* value of a dynamical system under study.

Finally, the third method of accomplishing the same task, deals with the entropy increase rates [5,6]. For large classes of dynamical systems, the rate of information loss in time is characterized by the Kolmogorov-Sinai (KS) entropy K_1, which is defined as the increase, per unit time, of the standard Boltzmann-Gibbs entropy $S_1 = -\sum_{i=1}^{W} p_i \ln p_i$, namely

$$K_1 \equiv \lim_{t\to\infty} \lim_{W\to\infty} \lim_{N\to\infty} \frac{S_1(t)}{t} \tag{4}$$

where t is the time, W is the number of regions in the partition of the phase space, N is the number of initial conditions (all chosen at $t = 0$ within one region among the W available ones) that are evolving in time. Although the KS entropy is defined, in principle, in terms of a single trajectory in phase space, it appears that, in almost all cases, it is possible to replace it by one based on an ensemble of initial conditions. The third method basically depends on the ensemble version of generalized KS entropy K_q, which has been introduced as the increase of a proper nonextensive entropic form, namely,

$$K_q \equiv \lim_{t\to\infty} \lim_{W\to\infty} \lim_{N\to\infty} \frac{S_q(t)}{t} \tag{5}$$

where S_q is the Tsallis entropy defined as [15]

$$S_q(t) = \frac{1 - \sum_{i=1}^{W} [p_i(t)]^q}{q-1} \tag{6}$$

where W is total number of configurations and $\{p_i\}$ are the associated probabilities. It is clear that, consistently, the well-known Pesin equality is also expected to be generalizable as $K_q = \lambda_q$ if $\lambda_q > 0$ and $K_q = 0$ otherwise. Within this scheme, it is conjectured that (i) a special q^* value exists such that K_q is finite for $q = q^*$, vanishes for $q > q^*$ and diverges for $q < q^*$; (ii) this special q^* value coincides with that coming from the two other distinct methods explained above. This also connects q^* values with the entropic index q of the Tsallis entropy as mentioned in [16]. At this point, it is worthwhile to clarify a subtlety related to the generalized Pesin equality: In fact, the q-generalized Pesin equality implies two things. Firstly, the values of q determined through the entropy rates are the same as those measured through other two distinct methods; secondly, the slopes of the entropy rates are the same as the generalized Lyapunov exponents of the sensitivity to the initial conditions. Throughout the present paper, we address and verify only the first point, not the second.

These three independent methods of obtaining q^* values have already been tested and verified with numerical calculations for a variety of one-dimensional dissipative (symmetric and asymmetric) map families [1–9], which strongly supports the idea that all these methods yield one and the same proper q^* value of a given map. On the other hand, up to now (to the best of our knowledge), there exist no attempt of testing these three methods in more general grounds like (i) two-(or more) dimensional dissipative maps, (ii) conservative maps, (iii) high dimensional dissipative and conservative systems. In this study, our aim is to analyze a two-dimensional dissipative map within these lines for the first time, which hopefully constitutes an important step forward as, we believe, it would presumably stimulate new efforts addressing the other general cases given above.

The two-dimensional map that we focus on here is the Henon map [17]

$$F(x,y) : \begin{pmatrix} x \\ y \end{pmatrix} \to \begin{pmatrix} 1 - ax^2 + y \\ bx \end{pmatrix} \tag{7}$$

where a and b are map parameters. This map reduces to the standard logistic map when $b = 0$, whereas it becomes conservative when $b = 1$, in between these two cases, it is a two-dimensional dissipative map.

Specifically, we focus on small values of the b parameter such as $b = 0.001$, 0.01, 0.1, etc since, for greater values of b, the numerical procedures used in the first and second methods do not allow us to analyze the map properly due to the increasing complexity of the system. To calculate the largest Lyapunov exponent of the system, among the numerical procedures like Benettin et al [18] or Froyland [19] algorithms, we use the procedure given in [20].

Before introducing our numerical findings of the three methods discussed above, let us recall our expectations. Since the Henon map, for all b values, belongs to the same universality class of the logistic map (namely, it has the same Feigenbaum numbers and box counting fractal dimension at the edge of chaos with the logistic map, irrespective of the b values, although the chaos threshold value a_c monotonically decreases for increasing b values), the natural expectation is to find a q^* value for the Henon map that coincides with the value of the logistic case ($q^* \simeq 0.24$) for all b values. However, since the verification of these three methods (employed so far to study only one-dimensional maps) in higher dimensional maps is quite valuable, it is better to use a test system with well known critical behaviour such as the Henon map. Within this reasoning, the present work will hopefully bring relevant information about the proper procedure to be used in investigating other high dimensional systems belonging to distinct universality classes.

First Method - Using the numerical procedure given in [20] for the calculation of the Lyapunov exponent, one can determine the time evolution of the sensitivity function. The procedure is the following: Using the derivative of the Henon map $DF(x, y)$, one can compute how an infinitesimally small error in a point (x, y) of the attractor is transformed by one iteration. For any arbitrary direction $(\cos(\phi), \sin(\phi))$ of the error, one can compute the transformed error using the equation

$$DF(x,y) \begin{pmatrix} \cos(\phi) \\ \sin(\phi) \end{pmatrix} = \begin{pmatrix} -2ax\cos(\phi) + \sin(\phi) \\ b\cos(\phi) \end{pmatrix} . \tag{8}$$

Therefore the error amplification is measured by the factor $[(-2ax\cos(\phi) + \sin(\phi))^2 + (b\cos(\phi))^2]^{1/2}$. By iteration and renormalizing this procedure one can obtain the largest Lyapunov exponent. As it is seen in Fig. 1, it exhibits a power-law divergence ($\xi \propto t^{1/(1-q^*)}$) at the edge of chaos and the upper bound slope of this fractal structure allows us to calculate the q^* value. For the (x_0, y_0) pairs, we use the numerically determined extremum values of x and its corresponding y values for each b parameter. For example, $(x_0, y_0) = (1, 0)$ for $b = 0$ (logistic case), $(x_0, y_0) = (1.0008451..., -0.0000001749...)$ for $b = 0.001$ and $(x_0, y_0) = (1.0084814..., -0.0000198735...)$ for $b = 0.01$. The values of critical a parameter calculated at the edge of chaos for some b values are the following: $a_c = 1.40115518...$ for $b = 0$, $a_c = 1.39966671...$ for $b = 0.01$ and $a_c = 1.38637288...$ for $b = 0.01$. From the analysis of Fig. 1, although the fractal structure and the slope seem to deteriorate with increasing values of b, this does not prevent us to conclude that the proper q^* value of the Henon map, for all b values, is $q^* \simeq 0.24$ since it is clearly seen that the fractal structure and the slope coincide with the logistic case ($b = 0$) for smaller time steps (in logarithmic scale) as b values increase, whereas they start to deteriorate for larger time step. As the values of b increase, the beginning of this deterioration shifts to smaller time steps. This originates from the fact that one needs a_c values with greater precision (in our calculations we have 10-11 digit precision) as b values increase, since the map becomes to be more complex. More precisely, this effect is the same as the one that we can face with even for the logistic map if lower precision is used for a_c value (for example, instead of 10-11 digit precision if one uses 6-7 digits for a_c, then a similar type of deterioration in the fractal structure is seen for smaller time steps for the logistic case as well). This point will become more transparent below when we discuss the second method in obtaining the proper q^* value of the Henon map.

Second Method - Now we turn our attention to the multifractal singularity spectrum $f(\alpha)$ of the critical attractor. If we can construct the $f(\alpha)$ curve for the Henon map, then it is evident from the scaling relation (3) that, using the end points of the spectrum, we can determine the proper q^* value of this map. Constructing the $f(\alpha)$ curve, we use the well-known procedure of Halsey et al. [13], however it is suitable here to mention that other algorithms such as Cvitanovic et al. [21] can also be used for this purpose. Before giving our results for the Henon map, we believe, it is better to reexamine the logistic map within this method in order to clarify the effect of precision of a_c values. To illustrate this point, in Fig. 2a we give three different cases for the logistic map. It is clearly seen that the $f(\alpha)$ curve obtained using high precision for a_c (circle) does not coincide with the one obtained using less precision for a_c

(dotted line) for the same number of iterations ($I = 1024$). On the other hand, we realize that it is possible to obtain the correct curve with less precision in a_c if smaller values of iteration numbers are used ($I = 256$) as it is evident from the Fig. 2a (full line). The same kind of behaviour for the $f(\alpha)$ curve has been observed for the Henon map as shown in Fig. 2b. Analyzing the results given in this figure, one can easily conclude that for the Henon map ($b \neq 0$) the precision of the a_c value used in calculations is not enough when larger number of iterations ($I = 1024$) is used, whereas the curve coincides with that of the logistic case (as expected) if smaller number of iterations is used ($I = 256$). It is worth mentioning that the correct value of box counting fractal dimension d_f of the critical attractor of the Henon map, which is the maximum value of the $f(\alpha)$ curve, is consistent with the above discussion (see Fig. 2). Therefore, within the light of this analysis, these results are quite convincing to conclude that the q^* value of the Henon map which comes from the second method is the same as the one obtained from the first method.

Third Method - Finally, we shall use the third method (i.e., entropy increase rate procedure) to estimate the proper q^* value of the Henon map in order to strengthen the results of the first and the second methods. To do this, we implement the following procedure [5,6] : firstly, we partition the phase space into W equal cells ($W = 1000 \times 1000$), then we choose one of these cells and select N initial conditions all inside this cell. As time evolves, these N points spread within the phase space, yielding a set of probabilities. In the beginning of time, naturally $S_q(0) = 0$, then the entropy increase rate gradually exhibits three successive regions. The entropy is almost constant in time in the first region, then it starts increasing in the second (intermediate) region and finally saturates in the third one. Among these regions, the intermediate one is the region where the linear increase of the proper entropy is expected to emerge [5,6]. Time evolution of $S_q(t)$ for the Henon map is given in Fig. 3. It is seen that, in the intermediate region, the linear increase of the entropy with time emerges only for a special value of q, and this value corresponds to the q^* value (within a good precision) determined previously from the other two methods. When $q \neq q^*$, the entropy curves upwards (if $q < q^*$) or downwards (if $q > q^*$). In order to quantitatively support this picture, we fit the curves with the polynomial $S_q(t) = A + Bt + Ct^2$ in the intermediate region $[t_1, t_2]$. Since the nonlinearity coefficient $R \equiv C(t_1 + t_2)/B$ is a measure of the importance of the nonlinear term, it should vanish for a strictly linear fit. In the inset of Fig. 3, we present the behaviour of R from where we estimate the proper value of q as $q^* = 0.25$, which is the value of the q index when R is strictly zero.

Summing up, we analyzed the mixing properties of a two-dimensional dissipative map at the edge of chaos using three distinct methods that are developed and tested so far for many one-dimensional map families. As being the first example that numerically verifies the scenario in two-dimensional maps, this work would hopefully stimulate new projects addressing more general cases like high dimensional dissipative and/or conservative dynamical systems. Along these lines, in an ongoing project which will be reported elsewhere, we analyze another two-dimensional map, the Lozi-type map [20], to provide additional support for the present scenario.

ACKNOWLEDGMENTS

Financial support of Turkish Academy of Sciences from the TUBA/GEBIP Program is acknowledged. I also thank Dr. Aziz-Alaoui for his invaluable help on the calculation of the Lyapunov exponents.

---

[1] C. Tsallis, A.R. Plastino and W.-M. Zheng, Chaos, Solitons and Fractals **8** (1997) 885.
[2] U.M.S. Costa, M.L. Lyra, A.R. Plastino and C. Tsallis, Phys. Rev. E **56** (1997) 245.
[3] M.L. Lyra and C. Tsallis, Phys. Rev. Lett. **80** (1998) 53.
[4] U. Tirnakli, C. Tsallis and M.L. Lyra, Eur. Phys. J. B **11** (1999) 309.
[5] V. Latora, M. Baranger, A. Rapisarda and C. Tsallis, Phys. Lett. A **273** (2000) 97.
[6] U. Tirnakli, G.F.J. Ananos and C. Tsallis, Phys. Lett. A **289** (2001) 51.
[7] U. Tirnakli, Phys. Rev. E **62** (2000) 7857.

[8] U. Tirnakli, Physica A **305** (2001) 119.
[9] U. Tirnakli, C. Tsallis and M.L. Lyra, Phys. Rev. E **65** (2002) 036207.
[10] P. Grassberger and M. Scheunert, S. Stat. Phys. **26** (1981) 697.
[11] T. Schneider, A. Politi and D. Wurtz, Z. Phys. B **66**, 469 (1987); G. Anania and A. Politi, Europhys. Lett. **7** (1988) 119.
[12] H. Hata, T. Horita and H. Mori, Progr. Theor. Phys. **82**, 897 (1989).
[13] T.C. Halsey et al, Phys. Rev. A **33** (1986) 1141.
[14] C. Beck and F. Schlogl, *Thermodynamics of chaotic systems* (Cambridge University Press, Cambridge, 1993)
[15] C. Tsallis, J. Stat. Phys. **52** (1988) 479.
[16] R.S. Johal and U. Tirnakli, e-print cond-mat/0201464.
[17] M. Henon, Comm. Math. Phys. **50** (1976) 69.
[18] G. Benettin, L. Galgani and J.M. Strelcyn, Phys. Rev A **14** (1976) 2338.
[19] J. Froyland, Phys. Lett. **97A** (1983) 8.
[20] M.A. Aziz-Alaoui, C. Robert and C. Grebogi, Chaos Solitons Fractals **12** (2001) 2323.
[21] P. Cvitanovic, G.H. Gunaratne and I. Procaccia, Phys. Rev. A **38** (1998) 1503.

Figure Captions

Figure 1 - Time evolution of the sensitivity function in a log-log plot for various values of b parameter.

Figure 2 - The behaviour of $f(\alpha)$ curve (a) for the logistic map, (b) for the Henon map.

Figure 3 - Time evolution of the Tsallis entropy for $b = 0.1$ for three different values of q. Inset: The nonlinearity coefficient R versus q. The interval characterizing the intermediate region is [7,19]. The dotted lines is guide to the eye.

Fig 1

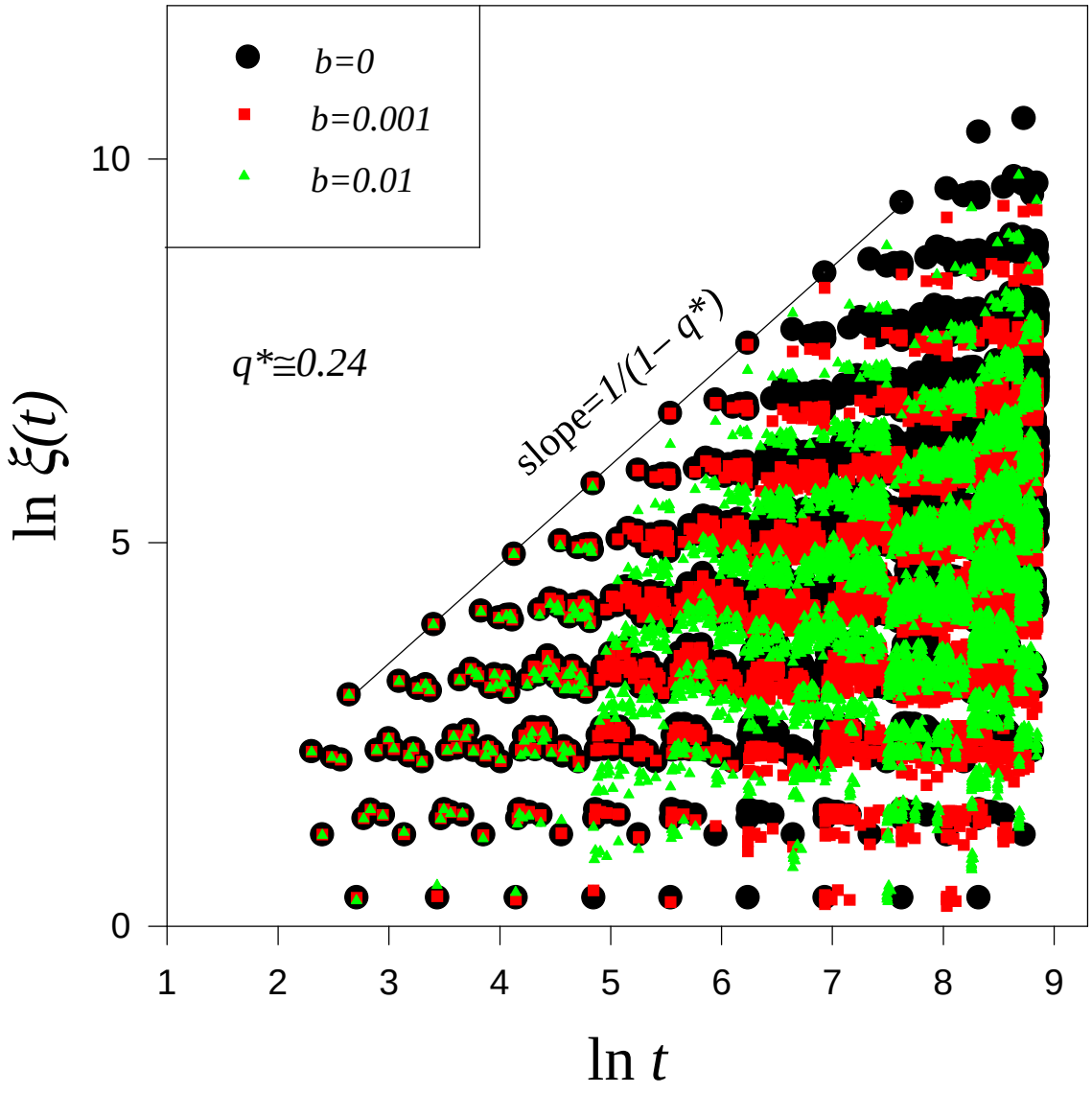

Fig 2

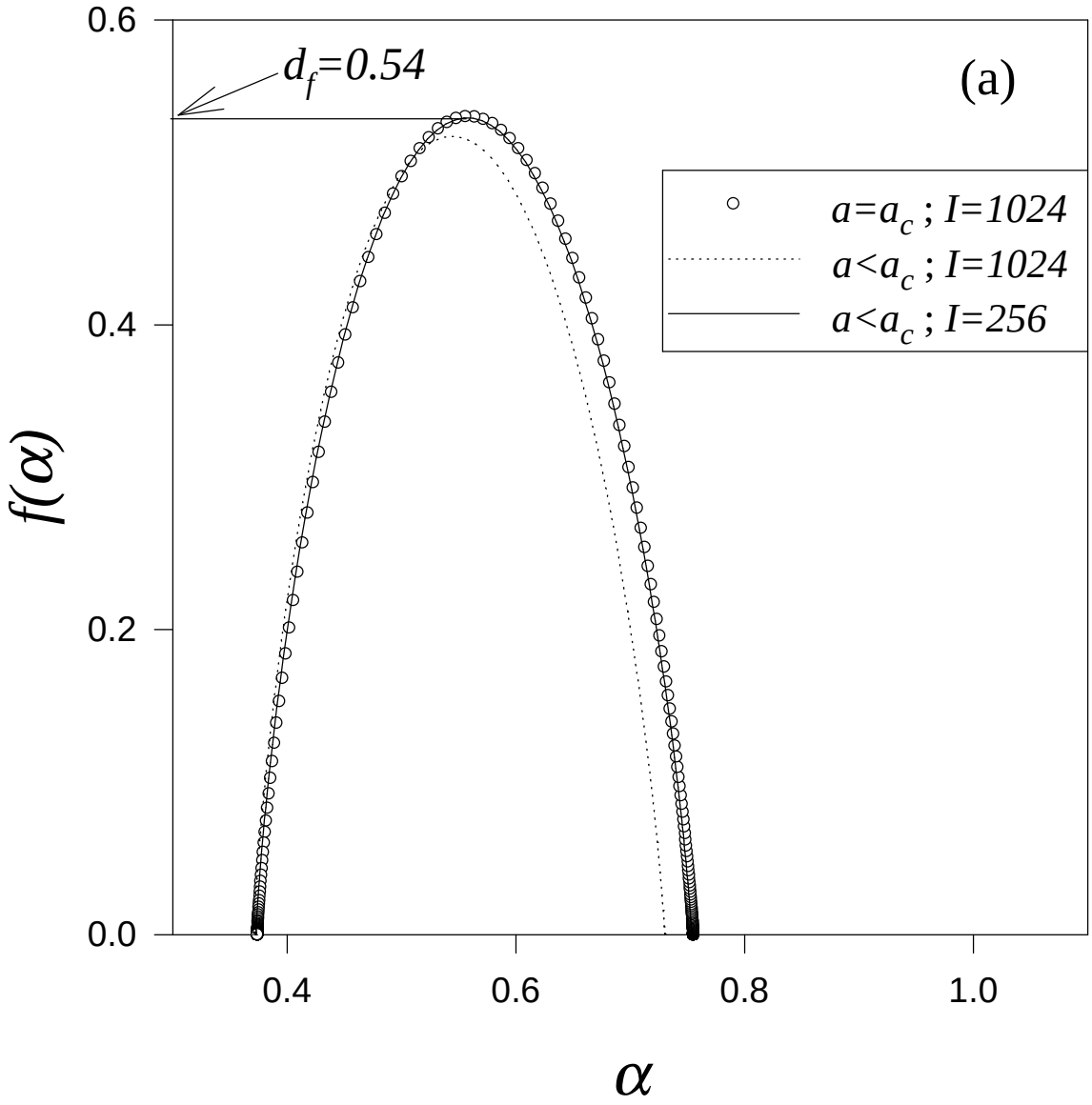
0.6
0.4
0.2
0.0
d_f=0.54
(a)
$a=a_c$; I=1024
$a<a_c$; I=1024
$a<a_c$; I=256
$f(\alpha)$
0.4
0.6
0.8
1.0
α

Fig 2

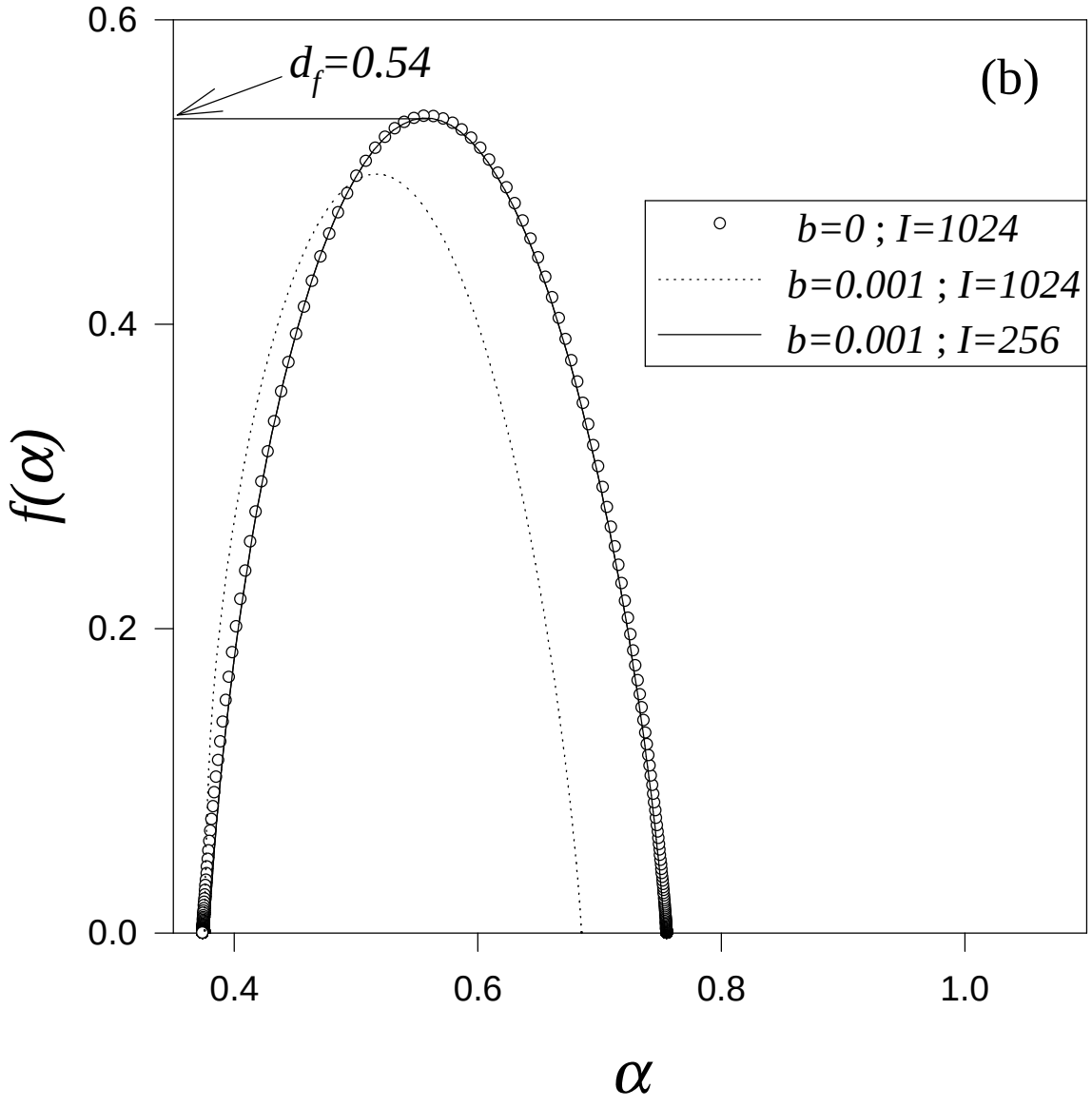
0.6
0.4
0.2
0.0
0.4
0.6
0.8
1.0
$f(\alpha)$
α
d_f=0.54
(b)
b=0 ; I=1024
b=0.001 ; I=1024
b=0.001 ; I=256

Fig 3

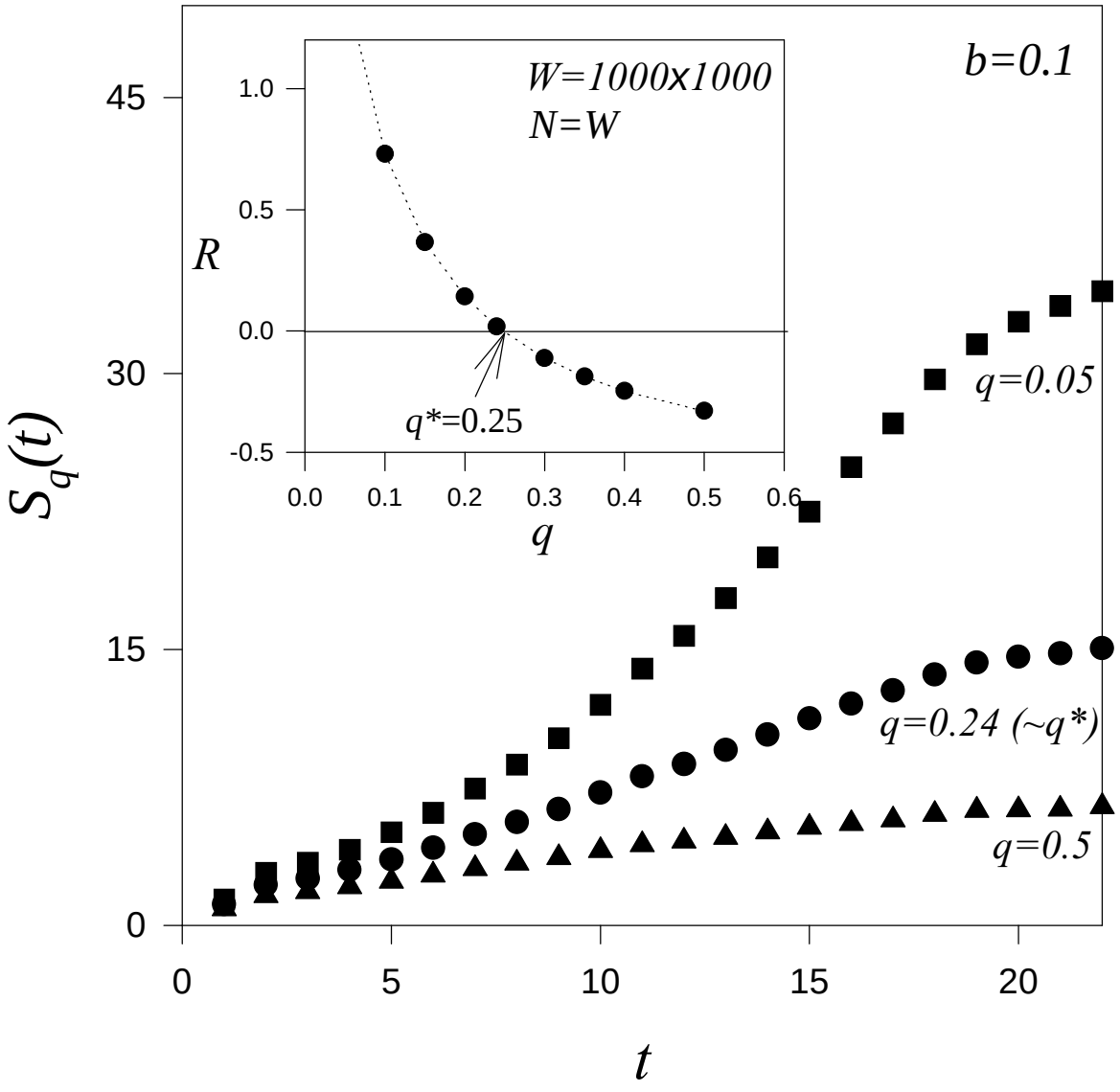
b=0.1
W=1000x1000
N=W
R
q*=0.25
q
q=0.05
q=0.24 (~q*)
q=0.5
$S_q(t)$
t
0
15
30
45
0
5
10
15
20
1.0
0.5
0.0
-0.5
0.0
0.1
0.2
0.3
0.4
0.5
0.6